Radiation-Induced Conductivity in Kapton-Like Polymers Featuring Conductivity Rising With an Accumulating Dose

Andrey Tyutnev, Vladimir Saenko, Aleksei Zhadov, and Evgenii Pozhidaev

***Abstract*— We have investigated the radiation-induced conductivity (RIC) in Kapton-like polymers in which it increases with an accumulating dose at large dose rates and long irradiation times. Such a behavior is very useful for spacecraft applications as it allows mitigating the spacecraft charging problems. Also, we studied ordinary polymers whose RIC steadily falls after reaching an initial maximum. To interpret experimental results, we used the semi-empirical Rose–Fowler–Vaisberg model. Numerical and experimental results have been compared with published data.**

***Index Terms*— Electrons, model calculations, polymer parameterization, polymers.**

I. Introduction

A GOOD understanding of charge accumulation dynamics in dielectrics subjected to the changing space radiative environments is required to ensure spacecraft operation reliability [1]. For this purpose, large facilities have been developed in these last decades to reproduce the complex spectra that may be encountered in the worst configurations of the space environment [2], and many experimental results have been obtained by recording the surface potential buildup on various polymer films subjected to an electron irradiation [3]–[6]. In these experiments, the value of the induced surface potential is determined by the competition of the charge accumulation and dissipation rate, the latter being due to surface secondary emission and radiation-induced conductivity (RIC).

Even for a constant dose rate, the intensity of RIC usually evolves with the irradiation time, and the mean charge depth may also change with time. This leads to a complex evolution of the potential, highly depending on the experimental conditions. It is thus almost impossible to rely on a purely empirical approach, and a physical model of the conduction processes in the insulator has to be developed.

The buildup of charge in an insulator subjected to an electron beam has been measured and modeled in the Faraday-cup technique in a shorted sample or by a voltage decay technique in an open surface geometry by B. Gross and co-workers from the early 1970s to the end of this century. The general overview of this last methodology has been recently given by G.M. Sessler *et al.* [7] (all close colleagues of the late B. Gross). Monoenergetic electron beams were used, and RIC was treated as an attendant phenomenon. The proposed RIC models suffered considerable simplification to fit the experimental results with RIC represented in its simplest form.

However, the voltage-decay method in an open surface geometry is not relevant for long time irradiations involving multienergetic beams [4]. The evolution of the material conductivity under irradiation has to be described using multiple trapping models [8], [9]. However, too many parameters are involved to allow their correct deduction by direct curve fitting of the surface potential data. Surface potential measurements as described above, corresponding to a realistic situation for spacecraft charging engineers, adds several layers of complexity to the already complex problem of RIC [10], [11]. The charge mean position and the electric field change with time in these experiments. RIC being usually highly field dependent, it is very difficult from the potential decay data to separate the phenomena [5].

The approach we present here consists in conducting bulk irradiations in a current-sensing mode, the time constant RC being much smaller than the observation time. The 1-D geometry of experiment is clearly preferable and the dose profile properly accounted for. In this approach, the RIC is the main and the only object of investigation. The chief proponent of this methodology was Hughes *et al.*. [12] working with PVK, PET, and SiO_2 and using latest radiation chemistry results combined with the multiple trapping formalism (see Refs. 4, 18, 19, and 66 in [8] and [12]). Our group used it from the very beginning (1982) until recently in line with the world trend in RIC studies as the only means to get the pertinent material parameters (see [8]).

Presently, the need to develop models based on an improved knowledge of RIC and charge carrier transport has indeed led other teams in the spacecraft charging community to introduce traditional RIC measurements to complement their surface potential measurements [6].

It is known that RIC in polymers under step-function and uniform irradiation initially rises to a maximum but then decreases continuously [8]. Such a behavior hinders removing an accumulating space charge and aggravates the situation with the electrostatic discharges [1]. In this respect, polymers with an appreciable RIC featuring nondecreasing behavior during irradiation are of special interest. Of these, the polyimide Kapton and polypyromellitimides generally should be noted [8].

Manuscript received September 6, 2018; revised December 4, 2018; accepted January 22, 2019. The review of this paper was arranged by Senior Editor H. B. Garrett. *(Corresponding author: Andrey Tyutnev.)*

The authors are with the Department of Electronic(al) Engineering, National Research University Higher School of Economics, 101000, Moscow, Russia (e-mail: aptyutnev@yandex.ru)

Color versions of one or more of the figures in this paper are available online at http://ieeexplore.ieee.org.

Digital Object Identifier 10.1109/TPS.2019.2901000

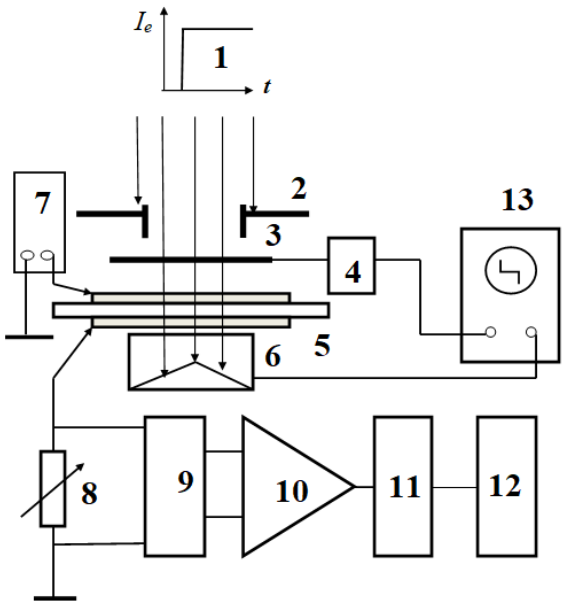

Fig. 1. Block diagram of the experimental set-up. (1) Electron beam in a pulse or continuous irradiation mode and its time profile. (2) Collimator. (3) Shutter. (4) Shutter control system. (5) Test sample. (6) Faraday cup to measure the penetrating electron current for controlling beam stability. (7) Power supply (up to 1200 V). (8) Set of resistors. (9) Electronic device protecting electronic instrumentation in the case of a sample breakdown. (10) Amplifier. (11) Analog-to-digital convertor. (12) Computer and a printer. (13) Oscilloscope.

II. Experimental Details

Investigated polymers included commercial films of the polyimide Kapton (25 μm thick) as well as its Russian analogues PM-1-OA (15 μm) and PM-1 (13 μm), polyethyleneterephthalate (PET, 8 μm), and polystyrene (PS, Styroflex, 20 μm). We also tested a representative of a new class of dielectric materials that have already found a wide application in the electrophotographic industry, namely, molecularly doped polymers (MDP). In our case, it was a bisphenol A polycarbonate doped with 30 wt.% of an aromatic hydrazone DEH [8]. Unlike other polymers tested, MDP samples approximately 20μm thick have been prepared in laboratory at Eastman Kodak Co. (USA). All specimens (40 mm in diameter) were supplied with evaporated Al electrodes 32 mm in diameter and 50 nm thick. We used only fresh samples for each experimental run.

Irradiations have been done with 50 keV electrons normally incident upon polymer samples inside a vacuum chamber of the ELA-65 electron gun at room temperature only (Fig. 1). The dose rate depth profile was typical for 50 keV electrons so that an average dose rate was estimated to be 2 times larger than at the front surface of a sample. RC time constant was about 1 ms.

Using a shutter (opening time 0.08 s) covered with a luminescent paint, it has been ascertained that the boundary of an irradiated spot was clear-cut. For a collimator 20 mm in diameter, it was found to be 30 mm in diameter, well inside Al electrodes. Exactly this area entered estimating the dose rate. To measure the beam current, we used the same shutter calibrated by the Faraday cup (for 50 keV electrons, the backscatter coefficient was estimated to be 11% in all polymers tested). The linear losses of 50-keV electrons were taken to be equal to 6.0 MeV cm^2/g as in PET [13] which has the same density and close average atomic weight as the polyimide Kapton. For the measured beam current of 110 nA, the average dose rate $R_0 = 190$ Gy/s in 25-μm-thick Kapton films as in all other polymers tested. During shutter opening, the dose rate increased almost linearly to a specified constant value. So, the step-function irradiation started at 0.1 s exactly. On all graphs time scale begins with the moment the shutter starts opening. To reduce the radiation-driven current (radiation pick-up) produced in a shorted sample by beam electrons stopping in the bulk, these electrons entered the sample through the high-voltage positively biased electrode. Since an applied voltage did not exceed 1.2 kV, the gained electrostatic energy (1.2 keV) was neglected compared with 50 keV acquired by electrons in the drifting space of the gun.

We estimate the accuracy of RIC absolute measurements as $\pm 30\%$ and relative ones as $\pm 10\%$. RIC data were presented as $\gamma_r(t) = j_r(t)/F_0$. Here, j_r is the current density and F_0 is the constant and uniform electric field.

In these studies, we used only fresh samples of the polyimide Kapton and PS cut from the same respective roll with a shelf life of about 35 years [14]. Samples cut from these polymer rolls were used intensively during all these years [8] We found that annealing dose effects in polyimides took 4 h in air at 120 C (in MDP 1 h at 65 C, also in air). After annealing, RIC curves were rather close to those registered in original samples (in our mobility studies in MDP, we used this property regularly [15]).

III. Experimental Results

A global picture of the RIC behavior for all polymers tested is presented on Fig. 2. We see that according to RIC behaviour, polymers clearly fall into two groups. PS and PET follow predictions of the Rose–Fowler–Vaisberg (RFV) model in that their RIC reaches an early maximum and then falls off during irradiation continuously [8]. In PS γ_r,(curve *3*) decreases as a power law $t^{-0.25}$ during irradiation from 0.2 s onward while in PET, it follows a more complicated decay pattern decreasing by a factor of 12 approximately during the 1-h irradiation session (in PS, this factor is about 10).

All other polymers follow theory predictions but only for an initial part of irradiation (a shallow dip is a clear evidence for this). Later on, their RIC begins to rise steadily with an accumulating dose as it happens in the polyimide Kapton. This behavior is especially pronounced in PM-1-OA and PM-1. The RIC in MDP seems to rise continuously grossly exceeding induced conductivity in all other polymers.

Fig. 2 demonstrates that an accumulating dose effect places an upper time limit for application of the standard RFV model while a shutter opening time limits the earliest time amenable to analysis to 0.1 s. These constraints forced us to take special measures to avoid any possible misinterpretation.

We see that all polyimides exhibit rather similar behavior. So, we concentrated on the polyimide Kapton currently widely studied elsewhere [3]–[6]. Also, we investigated for the first time the RIC of MDP. During past ten years, we extensively studied the hole transport in this polymer (see [15] and references therein) and its pulse RIC quite recently [16], [17].

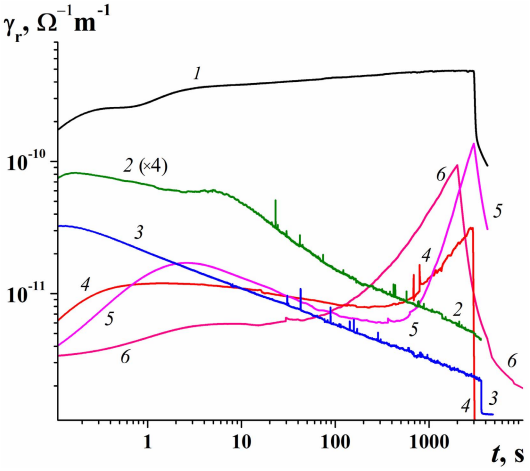

Fig. 2. RIC transients in polymers: (1) MDP. (2) PET. (3) PS. (4) Polyimide Kapton. (5) Polyimides PM-1-OA. (6) PM-1. Electric field 40 V/μm except 20 V/μm for (1). Dose rate 190 Gy/s. Accumulated dose was around 7×10^5 Gy. Values of curve 2 were multiplied by a factor of 4.

The main experimental information appears as the dose rate and field dependence of the maximum RIC $\gamma_{\rm rm}$:

$$\gamma_{\rm rm} = A_m R_0^{\Delta} \text{ and } \gamma_{\rm rm} \propto F_0^{\kappa} \qquad (1)$$

including the time t_m of its attainment.

Parameter A_m depends on the applied electric field in accord with the second of the above expressions.

There is yet another useful quantity characterizing the RIC and, namely, $\widehat{\varepsilon} = \gamma_{\rm rm} t_m/\varepsilon_0$ which directly concerns the prevailing recombination regime (ε_0 is the electrical constant). The RFV model predicts that $\gamma_{\rm rm} t_m = D(\alpha)\mu_0 e/k_r$ where $D(\alpha)$ is a numerical factor around unity [8]. The Langevin mechanism of the bimolecular recombination implies that $k_r = (e/\varepsilon\varepsilon_0)\mu_0$. Introducing the last formula into the preceding one, we find that $\widehat{\varepsilon}$ gets equal to $D(\alpha)\varepsilon$. As $D(\alpha) \leq 0.3$ for $\alpha \leq 0.3$ [8] and $\varepsilon \leq 3.4$ in all our polymers, we see the Langevin mechanism demands that $\widehat{\varepsilon}$ should be around unity.

Determination of Δ involved conductivity measurements at 1.9, 19, and 190 Gy/s. Assessing of κ was achieved by measuring RIC at two electric fields differing by two times. Thus, we found that increasing F_0 from 20 to 40 V/μm enhanced $\gamma_{\rm rm}$ (or the plateau in its region) in the polyimide Kapton by 1.6 times while the same effect in MDP has been achieved for a field change from 10 to 20 V/μm in good agreement with our earlier publications [14], [19]. These data mean that parameter κ is close to 0.7 for both polymers in the respective field regions. The most reliable information resulting from data processing of Figs. 3 and 4 is given in Table I.

It is seen that Δ in the polyimide Kapton is close to 0.95 while it is 0.7 in MDP. It is seen that RIC data for the polyimide Kapton agree rather satisfactorily with our previous results while those for the MDP are reported for the first time. Low values of $\widehat{\varepsilon}$ (around unity) testify in favor of the Langevin type of bimolecular recombination in both polymers. Note that our data for $\widehat{\varepsilon}$ in the polyimide Kapton argue for this mechanism more convincingly than in our previous work [8], [14]. The change of current buildup in a premaximum region in the polyimide Kapton (Fig. 3) is clearly observable and will be discussed in more detail in Section IV-A.

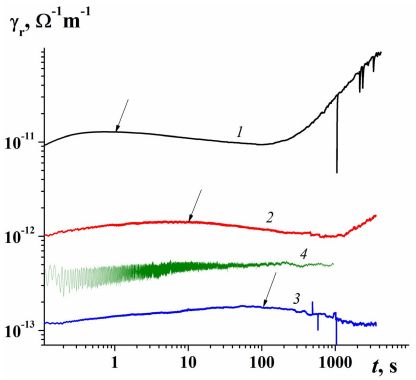

Fig. 3. RIC curves in the polyimide Kapton taken at (1) 190, (2) 19, (3) 1.9, and (4) roughly 0.3 Gy/s at 40 V/μm. Arrows indicate the position of the maximum RIC which are equal to 120 (1), 14 (2), and 1.7×10^{-13} Ω^{-1}m^{-1} (3). Values of curve 4 have been multiplied by a factor of 20.

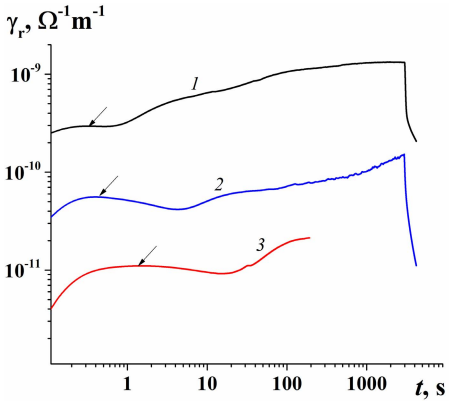

Fig. 4. RIC curves in the MDP taken for dose rates (1) 190, (2) 19, and (3) 1.9 Gy/s at 20 V/μm.

TABLE I

EXPERIMENTAL RIC DATA FOR THE POLYIMIDE KAPTON AND MDP TAKEN AT 40 AND 20 V/μM, RESPECTIVELY, FOR DOSE RATE 19 Gy/s. FOR $\gamma_{\rm RM}$, t_m, AND $\widehat{\varepsilon}$ DATA, REFER TO CURVE 2 IN FIGS. 3 AND 4

Parameter	Kapton		MDP
	This work	Source [14]	This work
Δ	0.95	0.82	0.7
γ_{rm}, Ω^{-1} m^{-1}	$1.4\text{x}10^{-12}$	$2.1\text{x}10^{-12}$	$5.5\text{x}10^{-11}$
A_m, Ω^{-1} m^{-1} (Gy^{-1} s)$^{\Delta}$	$0.85\text{x}10^{-13}$	$2.3\text{x}10^{-13}$	$0.7\text{x}10^{-11}$
t_m, s	10	18.4	0.4
$\widehat{\varepsilon}$	1.6	5.0	2.5

IV. RIC PARAMETERIZATION

To interpret experimental results we used the well-known RFV model that has been discussed at length quite recently [8].

The basic equations of the conventional one-carrier RFV model are as follows:

$$\begin{cases} \dfrac{dN}{dt} = g_0 - k_r N_0 N, \\ \dfrac{\partial \rho}{\partial t} = k_c N_0 \left[\dfrac{M_0}{E_1} \exp\left(-\dfrac{E}{E_1}\right) - \rho \right] - \nu_0 \exp\left(-\dfrac{E}{kT}\right) \rho \\ N = N_0 + \displaystyle\int_0^\infty \rho dE. \end{cases} \quad (2)$$

at $t = 0$ $N_0(t)$ and $\rho(E, t)$ are both zero.

By definition, the RIC is $\gamma_r(t) = e\mu_0 N_0(t)$. Thus, system (2) refers to unipolar (by tradition, electron) conduction.

Here, $N(t)$ is the total concentration of radiation-produced electrons (equal to that of holes). $N_0(t)$ is the concentration of mobile electrons in extended states (in transfer band) with microscopic mobility μ_0; g_0 is the generation rate of free charge carriers (assumed time and space independent during irradiation); k_r is the recombination coefficient of mobile electrons with immobile holes acting as recombination centers; k_c is the trapping rate constant; M_0 is the total concentration of traps exponentially distributed in energy E which is positive and taken downward from the energy level of the transport band; E_1 is the parameter of the trap distribution; $\rho(E, t)$ is the time dependent density distribution of trapped electrons; ν_0 is the frequency factor; T is temperature; k is Boltzmann's constant; and e is an elementary electric charge. Dispersive parameterα, which defines the major temporal features of the transient curves, is equal to kT/E_1. Also, $\tau_0 = (k_c M_0)^{-1}$ is the lifetime of mobile electrons before trapping. Of course, g_0 is proportional to the dose rate R_0 depending on the temperature and an applied electric field. In the case of hole conducting polymers, the roles of electrons and holes are to be swapped.

RIC generally consists of two components, the prompt γ_p and the delayed γ_d, both coexisting during irradiation. The former obeys first-order kinetics with a time constant in the sub nanosecond range scales with the dose rate. In the RFV model, the delayed component γ_d is found by solving (2) through the relationship

$$\gamma_d = \gamma_r - g_0 \mu_0 \tau_0 e \quad (3)$$

The prompt component should be inferred from experiment since the expression given by the RFV model $\hat{\gamma}_p = g_0 \mu_0 \tau_0 e$ usually differs markedly from its true value

$$\gamma_p = K_p R_0 \quad (4)$$

where parameter K_p is of universal nature weakly depending on temperature and an electric field. Now $(\gamma_d + \gamma_p)$ is to be compared with the experimentally registered RIC γ_r.

The RFV model predicts a simple relationship between $\alpha = kT/E_1$ and Δ under continuous step-function irradiation when bimolecular recombination comes fully into play (1) so that $\Delta = (1 + \alpha)^{-1}$ [8]. Shallow dips in experimental curves observed in Kapton and MDP are clear evidence to this. Our next task would be to explain quantitatively the observed values of $\gamma_{\rm rm}$ and t_m using the RFV model (see below).

A. Kapton

According to [16], K_p is approximately equal to 3.5×10^{-15} F/(m Gy). Earlier measurements using nanosecond 10 MeV electron pulses produced slightly different value 5×10^{-15} F/(m Gy) [20]. Now, studying the variation of the form of current decay immediately after the pulse end with the changing pulselength as outlined in [17] (this procedure is a tricky one and requires numerical calculations) it is possible to roughly evaluate the frequency factor. This procedure critically depends on the dispersion parameter α which is best assessed from studying the buildup and decay of the current curves. The RFV model predicts power-like buildup and decay curves for a small signal irradiation. The best analytical derivation of these power laws for an exponential trap distribution belongs to Arkhipov [18]. The power-like transients ($\gamma_d \propto t^{0.3}$ and $\gamma_d \propto t^{-0.8}$ for buildup and decay respectively) testify in favor of the exponential trap distribution with the dispersion parameter α lying between 0.2 and 0.3 [8]. Note that uncertainties do appear. Further numerical processing of pulse data requires α being close to 0.3 leading to $\nu_0 \approx 10^9$ s^{-1}. The quality of fitting pulse data may be judged by figures in round brackets in Table II. To quantify these data, one should assume the free ion yield $G_{\rm fi} = 0.77$ (40 V/μm, 295 K) as in [19] and $\mu_0 \tau_0 = 3 \times 10^{-16}$ m^2/V ($G_{\rm fi}$ is the number of free electron-hole pairs generated by 100 eV of absorbed energy).

TABLE II
PULSE DATA FOR THE POLYIMIDE KAPTON AT 40 V/μM. HERE, $\gamma_d(t_p)$ IS THE DELAYED CONDUCTIVITY MEASURED AT THE PULSE END AND $Q = \gamma_d(t_p)/\gamma_p$

Pulse length (t_p)	$\gamma_d(t_p) \cdot 10^{15}$, F/(m Gy)	Q	Source
40ns	$\approx$0.9	0.2-0.3 (0.33)	[20]
20 μ s	13	3.7 (4.2)	[17]
1 ms	60	14 (14)	[19]

It is only to be expected that these parameter values should be taken as initial in fitting RIC curves under continuous irradiation for not too long times thus minimizing effect of the accumulating dose. Details of the numerical calculations may be found elsewhere [21]. The purpose of the fitting procedure was to fit values of $\gamma_{\rm rm}$, t_m, and α.

In choosing the value of the dispersion parameter α, we had to reconcile its apparently different values for pulse and continuous irradiations. Indeed, analyzing pre-maximum parts of curves 2 to 4 on Fig. 3, we see that they clearly favor much smaller value about 0.08 as curves 2 and 3 demonstrate in the time interval less than $0.1t_m$. Indeed, in this time slot, current rises as a power law $t^{0.08}$. Analogous current behavior of curve 4 reveals even a milder time dependence $t^{0.06}$ which is badly obscured by the beam current instability at this low dose rate. So, we decided to use an intermediate value of the dispersion parameter 0.22 limiting our consideration to the one-parameter exponential trap distribution only. Nevertheless, this simplification allowed us to obtain an acceptable RIC description in a very broad time range extending from nanoseconds to about several seconds (curves 3 and 4 on Fig. 5).

The fitting parameters used in calculation of curve 2 on Fig. 5 are as follows: $\alpha = 0.22$, $\mu_0 = 10^{-5}$ m^2/ (V s), $\tau_0 = 0.7 \times 10^{-11}$ s ($\mu_0 \tau_0 = 0.7 \times 10^{-16}$ m^2/V), $\nu_0 = 10^9$ s^{-1}, $k_r = 2.6 \times 10^{-14}$ m^3 s^{-1} , $M_0 = 10^{26}$ m^{-3}. Also, it has been

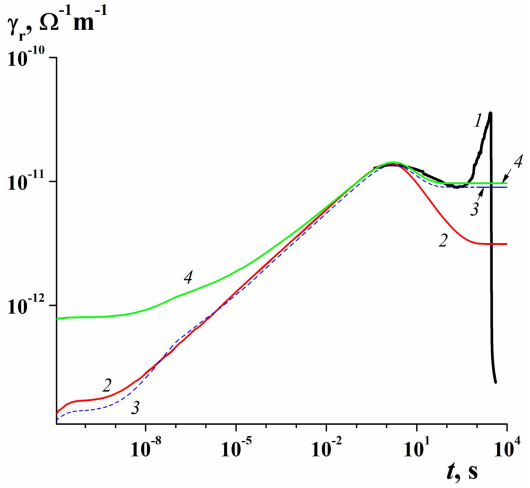

Fig. 5. Comparison of experimental (1, which is curve 1 on Fig. 2) and computed (2)–(4) RIC transients in the polyimide Kapton (see text for details). Dose rate 190 Gy/s, electric field 40 V/μm.

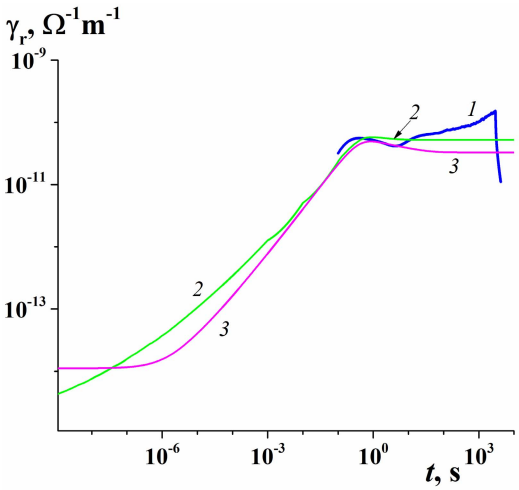

Fig. 6. Comparison of experimental (1, which is curve 2 on Fig. 3) and computed RIC transients in MDP in terms of (2) MTMg and (3) MTMe (see text for details). Dose rate 19 Gy/s, electric field 20 V/μm.

established that the best fit involves the free ion yield $G_{\rm fi} = 0.9$ which corresponds to the volume generation rate of free holes (and electrons) $g_0 = 1.5 \times 10^{22} {\rm m}^{-3}\ {\rm s}^{-1}$ for $R_0 = 190$ Gy/s as in experiment (see curve 1 on Fig. 5). This approach allowed us to reproduce experimental values of $\gamma_{\rm rm}$ and t_m.

But, at longer irradiation times, curve 2 starts to deviate appreciably from the experimental one (curve 1). Clearly, this approach overestimates recombination effect. In this situation, we had to modify the above one-carrier model by accounting for a bipolar conductivity in Kapton (there is a slight contribution of electrons) as in [17] and [21]. In the bipolar RFVmodel as developed in [21], this is achieved by introducing the bipolarity parameter χ which defines the relative conductivity due to electrons in relation to that of holes (majority carriers) in a small signal irradiation regime. Applying a numerical code developed in [21] and using $\chi = 0.1$ as in the cited work, we managed to improve fitting of the experimental data (compare curves 2 and 3 with curve 1 in the time range from 1 to 200 s). In doing so, we had to change τ_0 (0.58×10^{-11} s) which led to an insignificant drop of curve 3 at early times ($\leq 10^{-8}$ s).

We also made a correction for the real value of the prompt component in accordance with (3) and (4) (curve 4 on Fig. 5). It is seen that this correction has almost no effect at times exceeding t_m(curve 4 only slightly exceeds curve 3 in this time range).

Some more comments on Fig. 5. Curve 2 (red) was an initial attempt to fit an experimental curve 1. It overestimates recombination losses and starts to fall too fast. Curve 3 (dashed one) almost coinciding with curve 2 at times less than 0.1 s and nearly merging with curve 4 (green) at longer times accounting for the bipolar RIC in Kapton would have been the sought solution were it not for the presence of the prompt component of the RIC. This last sticking point has been successfully overcome as curve 4 demonstrates.

B. MDP

Contrary to the polyimide Kapton, an MDP like any other MDP is better described by the hopping Gaussian disorder model [22]–[25] properly simulated by the multiple trapping formalism with the Gaussian trap distribution (MTMg) [26]. In this approach, an exponential trap distribution appearing in (2) should be replaced with the Gaussian one ($E \geq 0$)

$$M(E) = \frac{M_0}{\sigma}\sqrt{\frac{2}{\pi}}\exp\left(-\frac{E^2}{2\sigma^2}\right). \tag{5}$$

Here, an energy parameter σ appears instead of E_1 in (2). Otherwise, a numerical code is the same.

To fit experimental data, we chose curve 2 on Fig. 4 as corresponding to the median value of the dose rate (19 Gy/s) which is enough to move $\gamma_{\rm rm}$ away from the shutter opening time. As indicated earlier, the MDP did not go through RIC studies and only once was pulse irradiated to examine the frequency factor field dependence [16], [17]. Unfortunately, the pulselength (20 μs) was too long to evaluate the RIC prompt component.

Our previous work with this MDP [15] provided initial information on MTMg parameters for the fitting procedure. Using multiple iterations, the following model parameters have been found: $\sigma = 0.13$ eV, $\mu_0 = 10^{-6}$ m^2/(V s), $\tau_0 = 1.9 \times 10^{-11}$ s, $\nu_0 = 3 \times 10^{10}$ s^{-1}, $k_r = 6 \times 10^{-15}$ m^3 s^{-1}, $M_0 = 10^{26}$ m^{-3}. Also, it has been established that the best fit involves free ion yield $G_{\rm fi} = 0.5$ at 20 V/μm which corresponds to volume generation rate $g_0 = 0.71 \times 10^{21}$ m^{-3} s^{-1} for $R_0 = 19$ Gy/s (as in experiment). Curve 2 (green) on Fig. 6 demonstrates the quality of the fitting: it successfully reproduces the value and timing of the maximum RIC but fails to secure a slight dip in RIC from 0.1 to approximately 30 s present in experimental curve 1 (blue) exhibiting instead a flat portion in the same region.

In this unsatisfactory situation, we tried also an exponential trap distribution (MTMe, which is identical to the RFV model). An iteration procedure recovered following model parameters: $\alpha = 0.75$, $\mu_0 = 10^{-5}$ m^2/(V s), $\tau_0 = 10^{-11}$ s, $\nu_0 = 10^6$ s^{-1}, $k_r = 6 \times 10^{-14}$ m^3 s^{-1}, $M_0 = 10^{26}$ m^{-3}. In this way, it became possible to account for a slight dip in RIC after maximum (curve 3 on Fig. 6). Like analogous situation in the polyimide Kapton, we ascribe its origin to the influence of the bimolecular recombination.

Curve 3 also manifests the presence of the prompt conductivity at short times (≤ 1 μs) approximately equal to 1.1×10^{-14} Ω^{-1} m^{-1} so that $K_p = 5.5 \times 10^{-16}$ F/(m Gy). In the case of MTMg, this parameter is even less as curve 2 on the same figure demonstrates. The real value of K_p is not known (according to [17], its upper limit is 3×10^{-15} F/(m Gy) and, to settle this issue, one needs to conduct additional nanosecond pulse measurements.

V. Dose-Modified RIC

Now, we address a peculiar RIC behavior in Kapton-like polymers (and MDP) at large accumulated doses still under irradiation The first step to unravel this unusual phenomenon was to compare conductivity curves taken at dose rates differing by orders of magnitude (Figs. 3 and 4). It is seen that the dose-modified (DM) RIC is definitely connected with long irradiations at high dose rates as observed in all polyimides starting at about at $t \approx 200$ s for $R_0 = 190$ Gy/s. The effect differs appreciably for different trademarks being especially pronounced in PM-1-OA. In the MDP, on the contrary, the DM-effect begins from the first seconds of irradiation and develops continuously, the starting time clearly increasing as dose rate diminishes.

An interesting observation about behavior of the DM-RIC in the polyimide Kapton comes from analyzing data presented on Fig. 3. It is seen that curves 1 and 2 are very similar as far as the long-time regions of these curves are concerned. Curves 3 and 4 are too short to visualize this effect but generally do not contradict this assertion. This means that DM-effect may be roughly assumed to be proportional to an accumulated dose.

The more detailed study of the DM-effect under conditions typical of the spacecraft operation in orbit needs appreciably longer irradiation times and respectively much lower dose rates than presently available with our experimental technique.

VI. Discussion

As far as we know, the DM RIC was first reported by researchers from Tomsk Polytechnic in 1977 [27] and subsequently intensively studied in Russia in middle 1980s [28]–[31]. Let us consider the main results of these early investigations.

The most conspicuous behavior of DM-RIC had been registered in PM-1 (the prime object of the above studies) which is synthesized through polycondensation of the diaminodiphenyl ether and the pyromellitic dianhydride. Once chemical structure of the dianhydride component is slightly changed, polyimide RIC behavior reverts to the norm (that is, the property of the DM-RIC disappears).

PM-1 films had been irradiated by 4- to 10-MeV protons in high vacuum (10^{-4} Pa) at room temperature. Dose rates were in the range 100–5000 Gy/s delivering doses up to 10^8 Gy. For accumulated doses up to 10^5 Gy, RIC behavior was quite normal, but then it started to rise by two or three orders of magnitude almost linearly in time. After irradiation end, the DM-RIC dropped to a value exceeding dark conductivity by several decades slowly relaxing to it allowing enough time to investigate this metastable state. Admitting air into the vacuum chamber immediately destroyed this effect.

It is interesting that DM-effect was also observed in electron high-intensity pulse irradiations [30]. For a mixture of PM-1 and 10 wt% polyorganosiloxane, we managed to produce DM-effect of the same intensity by electron irradiation to a dose of only 3×10^5 Gy and studied it in detail [31].

The overall conclusion is that DM-RIC occurs in polymers with a strong donor–acceptor interaction leading to the formation of a metastable conjugated structure easily destroyed by atmospheric oxygen. But this concept is still only a hypothesis that needs further development.

As we see, polymers with a strong MD-effect are well suited for spacecraft application like polyimides Kapton and PM-1-OA which are already widely used. The MDP still needs qualification tests. In this context, an introduction of dielectrics (polymers included) with intrinsic (dark) conductivity in vacuum of the order of 10^{-9} Ω^{-1} m^{-1} would solve the problem of in-orbit charging of dielectrics constituting thermal blankets and printed boards of the spacecraft electronics devices [32].

It would be interesting to compare our results with the results obtained by other teams investigating potential buildup on the same materials under irradiation. However, it is difficult to do it, since the RIC parameters we obtained in the work presented in this paper for the polyimide Kapton using the RFV model cannot be compared with the parameters reported in recent publications [3]–[6], [33], [34] using one- or two-trap models.

However, as mentioned earlier, the ONERA group has introduced the traditional RIC methodology (they call it a leakage current method) [6] to complement the existing surface potential technique.

In our previous paper [17], we came to the conclusion that the frequency factor in the polyimide Kapton should be increased to about 5×10^8 s^{-1} and as a result, the product $\mu_0 \tau_0$ should be lowered accordingly. Indeed, present results uniquely show that the best fitting of pulse as well as long-time irradiations demands this product be reduced from 3×10^{-16} to 0.7×10^{-16} m^2/V for $\nu_0 = 10^9$ s^{-1}. Also, we have introduced the Gaussian trap distribution into the modified RFV model for an MDP in line with the latest results in the field of charge carrier transport in MDP [8], [15].

VII. Conclusion

We have shown that DM-RIC is an intrinsic property of the Kapton-like polymers (and MDP) preventing their RIC from drastically falling at long irradiation times (and large accumulated doses) which is so characteristic of ordinary polymers like PET or PS. It has been speculated that the dose modified effect is due to the formation of the metastable conjugated structure *of an extended nature* in polymers already containing the well-defined side- or inner-chain molecular groups with local conjugation (the so-called chromophores) like polyvinylcarbazole and Kapton, respectively. In the MDP, these groups are present in the bulk as individual entities.

The aforementioned property is very useful for spacecraft application as it helps to control bulk charging of insulators used on outside spacecraft surfaces or as printed boards in electronics devices by electrons of the ambient space plasma. One must remember that this same function is even better served by "poor" dielectrics with their intrinsic (dark)

conductivity about 10^{-9} Ω^{-1} m^{-1} [32] being measured after long exposure in vacuum as recommended in [35] and [36]. Currently, dielectrics with a strong DM-effect should be considered as a palliative only in anticipation of their replacement with appropriate nanoconductive insulators tailor-made for the spacecraft industry.

One should be very careful making assessment of the RIC time, field, and temperature dependence using the surface potential decay technique. The RIC parameterization is highly recommended to be given in terms of the RFV model to allow direct comparison with published data.

ACKNOWLEDGEMENT

The authors would like to thank R. Ikhsanov for assessing bipolar effects in the polyimide Kapton (curves 3 and 4 on Fig. 5), and P. Molinie and T. Paulmier are gratefully acknowledged for their critical remarks. The authors would also like to thank D. Weiss for supplying MDP samples. They would also like to thank the Basic Research Program of the National Research University Higher School of Economics, Moscow, for their support.

REFERENCES

[1] H. B. Garrett and A. C. Whittlesey, "Spacecraft charging, an update," *IEEE Trans. Plasma Sci.*, vol. 28, no. 6, pp. 2017–2028, Dec. 2000.

[2] T. Paulmier, B. Dirassen, M. Belhaj, V. Inguimbert, D. Payan, and N. Balcon, "Experimental test facilities for representative characterization of space used materials," in *Proc. 14th ESA/ESTEC SCTC*, Noordwijk, The Netherlands, Apr. 2016, pp. 4–8.

[3] T. Paulmier, B. Dirassen, D. Payan, and M. van Eesbeek, "Material charging in space environment: Experimental test simulation and induced conductive mechanisms," *IEEE Trans. Dielectr. Electr. Insul.*, vol. 16, no. 3, pp. 682–688, Jun. 2009.

[4] P. MolinieÌ' *et al.*, "Polyimide and FEP charging behavior under multi-energetic electron-beam irradiation," *IEEE Trans. Dielectr. Electr. Insul.*, vol. 19, no. 4, pp. 1215–1220, Aug. 2012.

[5] T. A. Paulmier, A. Sicard-Piet, D. Lazaro, M. Arnaout, and D. Payan, "Analysis of charging kinetics on space dielectrics under representative worst case geostationary conditions," *IEEE Trans. Plasma Sci.*, vol. 43, no. 9, pp. 2849–2855, Sep. 2015.

[6] T. Paulmier, B. Dirassen, D. Payan, and M. Arnaout, "Analysis of charge transport and ionization effect in space-used polymers under high-energy electron irradiation," *IEEE Trans. Plasma Sci.*, vol. 45, no. 8, pp. 1933–1937, Aug. 2017.

[7] G. M. Sessler, M. T. Figueiredo, and G. F. L. Ferreira, "Models of charge transport in electron-beam irradiated insulators," *IEEE Trans. Dielectr. Electr. Insul.*, vol. 11, no. 2, pp. 192–202, Apr. 2004.

[8] A. P. Tyutnev, V. S. Saenko, E. D. Pozhidaev, and R. S. Ikhsanov, "Experimental and theoretical studies of radiation-induced conductivity in spacecraft polymers," *IEEE Trans. Plasma. Sci.*, vol. 43, no. 9, pp. 2915–2924, Sep. 2015.

[9] P. Molinié, "A panorama of electrical conduction models in dielectrics, with application to spacecraft charging," *IEEE Trans. Plasma Sci.*, vol. 43, no. 9, pp. 2869–2874, Sep. 2015.

[10] R. Hanna *et al.*, "Characterization of charge carrier lateral conduction in irradiated dielectric materials," *J. Phys. D: Appl. Phys.*, vol. 44, Oct. 2011, Art. no. 445402.

[11] R. Hanna *et al.*, "Radiation induced conductivity in space dielectric materials," *J. Appl. Phys.*, vol. 115, Jan. 2014, Art. no. 033713.

[12] R. C. Hughes, "Electronic and ionic charge carriers in irradiated single cystal and fused quartz," *Radiat. Effects*, vol. 26, no. 4, pp. 225–235, 1975.

[13] L. Pages, E. Bertel, H. Joffre, and L. Sclavenitis, "Energy loss, range, and bremsstrahlung yield for 10-keV to 100-MeV electrons in various elements and chemical compounds," *At. Data Nucl. Data Tables*, vol. 4, pp. 1–127, Mar. 1972.

[14] A. P. Tyutnev *et al.*, "Radiation-induced conductivity in polymers under continuous irradiation," (in Russian), *Khim. Vysok. Energii*, vol. 27, no. 2, pp. 32–38, 1993.

[15] A. P. Tyutnev, D. S. Weiss, D. H. Dunlap, and V. S. Saenko, "Time-of-flight current shapes in molecularly doped polymers: Effects of sample thickness and irradiation side and carrier generation width," *J. Phys. Chem. C*, vol. 118, pp. 5150–5158, Feb. 2014.

[16] A. P. Tyutnev and V. S. Saenko, "Poole-Frenkel mobility field dependence in molecularly doped polymers revisited," *Chem. Phys.*, vols. 483–484, pp. 172–176, Feb. 2017.

[17] A. Tyutnev, V. Saenko, and E. Pozhidaev, "Frequency factor of the semiempirical model for the radiation-induced conductivity in spacecraft polymers," *IEEE Trans. Plasma Sci.*, vol. 46, no. 3, pp. 645–650, Mar. 2018.

[18] V. I. Arkhipov, "An adiabatic model of trap-controlled dispersive transport and recombination," *J. Non-Cryst. Solids*, vol. 163, no. 3, pp. 274–282, 1993.

[19] A. P. Tyutnev, R. S. Ikhsanov, K. V. Marchenkov, V. S. Saenko, and E. D. Pozhidaev, "Dose effects in radiation-induced conductivity of polypyromellitimide," *Polym. Sci. A*, vol. 50, no. 4, pp. 429–433, 2008.

[20] A. P. Tyutnev, V. N. Abramov, P. I. Dubenskov, V. S. Saenko, A. V. Vannikov, and E. D. Pozidaev, "Time-resolved nanosecond radiation-induced conductivity in polymers," *Acta Polym.*, vol. 37, no. 6, pp. 336–342, 1986.

[21] A. P. Tyutnev, R. S. Ikhsanov, V. S. Saenko, and E. D. Pozhidaev, "Theoretical analysis of the Rose-Fowler-Vaisberg model," *Polym. Sci. A*, vol. 49, no. 7, pp. 861–866, 2007.

[22] H. Bässler, "Charge transport in disordered organic photoconductors a Monte Carlo simulation study," *Phys. Status Solid B*, vol. 175, no. 1, pp. 15–56, 1993.

[23] P. M. Borsenberger and D. S. Weiss, *Organic Photoreceptors for Xerography*. New York, NY, USA: Marcel Dekker, 1998.

[24] V. R. Nikitenko, H. von Seggern, and H. Bässler, "Non-equilibrium transport of charge carriers in disordered organic materials," *J. Phys., Condens. Matter*, vol. 19, no. 13, pp. 136210-1–136210-15, 2007.

[25] V. R. Nikitenko and M. N. Strikhanov, "Transport level in disordered organics: An analytic model and Monte-Carlo simulations," *J. Appl. Phys.*, vol. 115, no. 7, 2014, pp. 073704-1–073704-9.

[26] A. Tyutnev, R. Ikhsanov, V. Saenko, and E. Pozhidaev, "Analysis of the carrier transport in molecularly doped polymers using the multiple trapping model with the Gaussian trap distribution," *Chem. Phys.*, vol. 404, pp. 88–93, Aug. 2012.

[27] A. V. Shelenin, private communication, 1977.

[28] O. G. Kazakov and V. P. Sichkar, "Dose effects in radiation-induced conductivity of polymers," (in Russian), *Plast. Massy*, vol. 7, no. 3, pp. 46–48, 1980.

[29] A. P. Tyutnev, V. S. Saenko, V. S. Tikhomirov, and Y. D. Pozhidaev, "Radiation impulse induced electrical conductivity of aromatic polymides with dianhydride components of differing structure," *Polym. Sci. A*, vol. 25, no. 1, pp. 113–122, 1983.

[30] A. P. Tyutnev *et al.*, "Dose effects in transient radiation-induced conductivity in polymers," *Phys. Status Solid A*, vol. 89, no. 1, pp. 311–320, 1985.

[31] A. P. Tyutnev, S. G. Boev, and D. N. Sadovnichii, "On a new mechanism of radiation-induced conductivity in polymers with strong donor-acceptor interaction," *High Energy Chem.*, vol. 28, no. 2, pp. 103–105, 1994.

[32] V. Saenko, A. Tyutnev, A. Abrameshin, and G. Belik, "Computer simulations and experimental verification of the nanoconductivity concept for the spacecraft electronics," *IEEE Trans. Plasma Sci.*, vol. 45, no. 8, pp. 1843–1846, Aug. 2017.

[33] R. Pacaud, T. Paulmier, and P. Sarrailh, "1-D physical model of charge distribution and transport in dielectric materials under space radiations," *IEEE Trans. Plasma Sci.*, vol. 45, no. 8, pp. 1947–1954, Aug. 2017.

[34] K. A. Ryden and A. D. P. Hands, "Modeling of electric fields inside spacecraft dielectrics using in-orbit charging current data," *IEEE Trans. Plasma Sci.*, vol. 45, no. 8, pp. 1927–1932, Aug. 2017.

[35] A. R. Frederickson, C. E. Benson, and J. F. Bockman, "Measurement of charge storage and leakage in polyimides," *Nucl. Instrum. Methods Phys. Res. B, Beam Interact. Mater. At.*, vol. 208, pp. 454–460, Aug. 2003.

[36] J. R. Dennison, J. Brunson, P. Swaminathan, N. W. Green, and A. R. Frederickson, "Methods for high resistivity measurements related to spacecraft charging," *IEEE Trans. Plasma Sci.*, vol. 34, no. 5, pp. 2191–2203, Oct. 2006.

Authors' photographs and biographies not available at the time of publication.